Available online at www.sciencedirect.com
SCIENCE DIRECT®
PERGAMON
Polyhedron 22 (2003) 2821–2830
POLYHEDRON
www.elsevier.com/locate/poly

Structural, thermal, and magnetic properties of three transition metal-4,4′-bipyridine coordination polymers: $[Ni(4,4'\text{-bipy})_3(H_2O)_2](ClO_4)_2\cdot 1.4(4,4'\text{-bipy})\cdot 3(H_2O)$; $[Co(4,4'\text{-bipy})_3(H_2O)_2](ClO_4)_2\cdot 1.4(4,4'\text{-bipy})\cdot 3(H_2O)$; $[Cu(4,4'\text{-bipy})_3(DMSO)_2](ClO_4)_2\cdot 2(4,4'\text{-bipy})$

Jonathan D. Woodward [a], Rénal Backov [a], Khalil A. Abboud [a], Hitoshi Ohnuki [b], Mark W. Meisel [b], Daniel R. Talham [a,*]

[a] Department of Chemistry, University of Florida, Gainesville, FL 32611-7200, USA
[b] Department of Physics and Center for Condensed Matter Sciences, University of Florida, Gainesville, FL 32611-8440, USA

Received 6 March 2003; accepted 17 June 2003

Abstract

Three new transition metal coordination polymers based on 4,4′-bipyridine (4,4′-bipy) are reported. The reaction of 1 equiv. of nickel(II) perchlorate hexahydrate or cobalt(II) perchlorate hexahydrate with 3 equiv. of 4,4′-bipy under inert atmosphere, hydrothermal conditions yields $[Ni(4,4'\text{-bipy})_3(H_2O)_2](ClO_4)_2\cdot 1.4(4,4'\text{-bipy})\cdot 3(H_2O)$ (**1**) and the isostructural $[Co(4,4'\text{-bipy})_3(H_2O)_2](ClO_4)_2\cdot 1.4(4,4'\text{-bipy})\cdot 3(H_2O)$ (**2**), respectively, while the combination of one equivalent of copper(II) perchlorate hexahydrate with three equivalents of 4,4′-bipy under ambient laboratory conditions in dimethyl sulfoxide produces the structurally related $[Cu(4,4'\text{-bipy})_3(DMSO)_2](ClO_4)_2\cdot 2(4,4'\text{-bipy})$ (**3**). The metal:bipy molar ratio within the framework is 1:3 for each structure. Each sample consists of coordinate covalent metal-(4,4′-bipy) chains that pack through a combination of weaker hydrogen bonding and π-stacking interactions to form two-dimensional sheets. The sheets in turn pack to form three-dimensional structures with oblique channels that extend throughout the solid and contain enclathrated guest molecules. All three samples are susceptible to loss of enclathrated guest molecules. Magnetic data indicate that each sample behaves essentially Curie-like, with only small exchange coupling ($J/k_B < 1$ K) observed in each case.

Keywords: Coordination polymers; Crystal structures; Transition metal ions; 4,4′-bipyridine; Network solids

1. Introduction

The bidentate ligand, 4,4′-bipyridine (4,4′-bipy), is a commonly employed spacer in the synthesis of coordinate-covalent network solids, and a number of coordination polymers incorporating this ligand with different network architectures in the solid-state have been reported [1–9]. Examples that form one-dimensional chains include $[Co(SO_4)(H_2O)_3(4,4'\text{-bipy})]\cdot 2(H_2O)$ [10], [Ni(Et-XA)$_2$(4,4′-bipy-)]·0.5(EtOH)·($CHCl_3$) (Et-XA = ethylcarbonadithiolate) [11], $[Co(NCS)_2(H_2O)_2(4,4'\text{-bipy})]\cdot(4,4'\text{-bipy})$ [12], and [Mn(hfac)$_2$(4,4′-bipy)] (hfac = hexafluoroacetylacetonato) [13], while $[Ni(4,4'\text{-bipy})_{2.5}(H_2O)_2](ClO_4)_2\cdot 1.5(4,4'\text{-bipy})\cdot 2(H_2O)$ [9] and $[Co(4,4'\text{-bipy})_{1.5}(NO_3)_2]\cdot$guest (guest = MeCH or $CHCl_3$) [5] form railroad and ladder-like structures, respectively. Examples that form two-dimensional grids or sheets include $[Cd(4,4'\text{-bipy})_2(NO_3)_2]\cdot 2(C_4H_6Br_2)$ [1], $[Cu(4,4'\text{-bipy})(H_2O)_2(FBF_3)_2]\cdot(4,4'\text{-bipy})$ [14], $[Co(NCS)_2(4,4'\text{-bipy})_2]\cdot 2(CH_3CH_2)_2O$ [12], [M(4,4′-bipy)(ox)] (M = Fe(II), Co(II), Ni(II), and Zn(II) and ox = oxalato) [2] and $[M(4,4'\text{-bipy})_2(H_2O)_2](ClO_4)_2\cdot$guest (M = Cu, Zn, and Cd and guest = enclathrated guest molecule) [15].

* Corresponding author. Tel.: +1-352-392-9016; fax: +1-352-392-3255.
E-mail address: talham@chem.ufl.edu (D.R. Talham).

0277-5387/03/$ - see front matter © 2003 Elsevier Ltd. All rights reserved.
doi:10.1016/S0277-5387(03)00409-1

This paper reports the crystal structures, thermal behavior, and magnetic properties of a series of three linear chain compounds containing the 4,4′-bipy spacer that organize in the solid state to form new non-interpenetrated network solids. The compounds $[Ni(4,4'\text{-bipy})_3(H_2O)_2](ClO_4)_2\cdot 1.4(4,4'\text{-bipy})\cdot 3(H_2O)$ (**1**), $[Co(4,4'\text{-bipy})_3(H_2O)_2](ClO_4)_2\cdot 1.4(4,4'\text{-bipy})\cdot 3(H_2O)$ (**2**) and $[Cu(4,4'\text{-bipy})_3(DMSO)_2](ClO_4)_2\cdot 2(4,4'\text{-bipy})$ (**3**) were each prepared by the direct combination of 3 equiv. of 4,4′-bipy with 1 equiv. of their respective metal ion. Compounds **1** and **2** are isostructural and were crystallized under inert atmosphere hydrothermal conditions. The related structure **3** was isolated under ambient laboratory conditions from dimethyl sulfoxide. All three materials share a common structural motif with one-dimensional, covalently linked chains interacting via hydrogen bonding and π-stacking forces to form layered sheets with characteristic hydrophobic, rectangular cavities. These sheets are packed in a manner that aligns the cavities to form oblique channels occupied by enclathrated guest molecules and counterions that extend throughout the solid. The thermal instability of these coordination polymers is associated with the relatively low temperatures at which the guest molecules are lost. Temperature and field dependent magnetization measurements revealed weak magnetic coupling between the paramagnetic metal centers, as 4,4′-bipy is a poor mediator of superexchange interactions [11,13,16].

2. Experimental

2.1. Materials

Copper(II) perchlorate hexahydrate (98%), cobalt(II) perchlorate hexahydrate (98%), nickel(II) perchlorate hexahydrate (98%), 4,4′-bipyridine (98%), and sodium azide were purchased from Aldrich (Milwaukee, WI). Dimethylsulfoxide (99.9%) was purchased from Fisher Scientific (Pittsburgh, PA). Ethanol (100%) was purchased from Aaper Chemical (Shelbyville, KY). All reagents were used without further purification. Elemental analyses were performed by the University of Florida Spectroscopic Services laboratory.

Caution: perchlorate salts of metal complexes with organic ligands are potentially explosive. While we have not observed explosive decomposition of this compound in studies up to 250 °C, caution should be exercised when handling perchlorate salts.

2.2. Synthesis of $[Ni(4,4'\text{-bipy})_3(H_2O)_2](ClO_4)_2\cdot 1.4(4,4'\text{-bipy})\cdot 3(H_2O)$ (**1**)

A solution was prepared by dissolving 731 mg of $Ni(ClO_4)_2\cdot 6H_2O$ (2.00×10^{-3} mol) in 10 ml of water contained within a Teflon canister. Addition of 934 mg of 4,4′-bipyridine (6.00×10^{-3} mol) and 2 ml of ethanol to this solution resulted in a blue–green colored suspension. This canister was in turn sealed within a homemade, stainless steel hydrothermal vessel, purged with argon gas, and heated to 150 °C for 5 days. The container was subsequently cooled to room temperature (r.t.) over a period of 24 h without any specific control over the rate of cooling. The resulting blue–green crystals, obtained in 88% yield (based on initial quantity of bipy), were washed with water before further characterization. The crystals become opaque within a few hours upon removal from the solvent. *Anal.* Calc. for $NiC_{44}H_{45.8}N_{8.8}O_{13}Cl_2$: C, 51.66; H, 4.48; N, 12.05. Found: C, 50.88; H, 4.47; N, 12.14%.

2.3. Synthesis of $[Co(4,4'\text{-bipy})_3(H_2O)_2](ClO_4)_2\cdot 1.4(4,4'\text{-bipy})\cdot 3(H_2O)$ (**2**)

Using the same procedure described for **1**, 731 mg of $Co(ClO_4)_2\cdot 6H_2O$ (2.00×10^{-3} mol) was reacted with 934 mg of 4,4′-bipyridine (6.00×10^{-3} mol) in 10 ml of water with 2 ml of ethanol at 150 °C for 3 days. The resulting orange crystals, obtained in 92% yield (based on initial quantity of bipy), were washed with water before further characterization. The crystals become opaque within a few hours upon removal from the solvent. *Anal.* Calc. for $CoC_{44}H_{45.8}N_{8.8}O_{13}Cl_2$: C, 51.65; H, 4.48; N, 12.04. Found: C, 50.87; H, 4.47; N, 12.14%.

2.4. Synthesis of $[Cu(4,4'\text{-bipy})_3(DMSO)_2](ClO_4)_2\cdot 2(4,4'\text{-bipy})$ (**3**)

A solution containing 741 mg of $Cu(ClO_4)_2\cdot 6\ H_2O$ (2.00×10^{-3} mol) dissolved in 10 ml of DMSO was combined with a solution containing 934 mg of 4,4′-bipyridine (6.00×10^{-3} mol) dissolved in 10 ml of DMSO. The resulting dark blue colored mixture, contained within an evaporating dish, initially produced small, blue, block-like crystals within 2 weeks of solvent evaporation. Within and additional four weeks, light blue colored hexagonal plates of **3** were isolated and washed with DMSO before further characterization. The composition was determined by X-ray structure analysis.

2.5. X-ray structure determination

A blue–green crystal of **1** ($0.25\times0.23\times0.23$ mm^3), an orange crystal of **2** ($0.51\times0.36\times0.17$ mm^3), and a blue crystal of **3** ($0.24\times0.21\times0.12$ mm^3) were selected for X-ray analysis. Each crystal was mounted on a glass fiber under nitrogen gas. The same data collection procedure was used for each sample. Data were collected at 173 K on a Siemens SMART PLATFORM equipped with a CCD area detector and a graphite monochromator. Cell parameters were refined using up

to 8192 reflections. A full sphere of data (1850 frames) was collected using the ω-scan method (0.3° frame width). The first 50 frames were re-measured at the end of data collection to monitor instrument and crystal stability (maximum correction on I was $<1\%$). Absorption corrections by integration were applied based on measured indexed crystal faces.

The structures were solved by the direct methods in SHELXTL6 and refined using full-matrix least-squares [17]. The non-H atoms were treated anisotropically, whereas the hydrogen atoms were calculated in ideal positions by riding on their respective carbon atoms. The H atoms from the coordinated water molecules were found and refined. The uncoordinated 4,4′-bipyridine molecules and perchlorate anions are disordered in each structure. In **1** and **2**, two half-bipy guest moieties are each disordered about a center of inversion. The perchlorate anions are disordered in four parts but the oxygen atoms on only two major components were found in Difference Fourier maps and refined anisotropically. Only the Cl atoms of the minor disordered parts were found and refined. Additionally, one of these (occupation factor is 0.2) occupies common space with another half bipy (occupation factor is 0.2). Thus, the total number of guest bipy per formula, 1.4, obtained upon doubling the asymmetric unit is $2\times(0.5+0.2)$.

In **3**, a single guest 4,4′-bipy has one pyridyl ring disordered. The S atom of one coordinated DMSO molecule is disordered as well. The site occupation factors of the disordered parts were dependently refined to 0.88(1) for the major part and consequently 0.12(1) for the minor part; S′ was refined with an isotropic thermal parameter. For both perchlorate anions, disorder was found each in two positions and their site occupation factors were dependently refined to 0.69(1) and 0.31(1) for one anion, and 0.50(1) for each part of the second disordered anions. A total of 428 and 427 parameters were refined employing F^2 in the final cycle using 4328 and 4393 reflections with $I>2\sigma(I)$.

2.6. Thermal analysis

Thermogravimetric analyses (TGA) of the title compounds were performed on a computer-controlled TA Instruments Hi Res TGA 2950 thermogravimetric analyzer. Powdered samples of **1** (4.5740 mg), **2** (3.7460 mg), and **3** (6.3730 mg) were loaded into alumina pans and heated with a ramp rate of 10 °C min^{-1} from r.t. to 600 °C. Thermal desorption mass spectrometry measurements were recorded on a MAT 95 utilizing electron ionization techniques. Crystalline samples, contained within capillary tubes, were evacuated, loaded into direct insertion probes, and heated with a ramp rate of 10 °C min^{-1} from 30 to 400 °C.

2.7. Magnetic measurements

Bulk magnetization measurements were obtained from a standard Quantum Design MPMS SQUID magnetometer. The samples consisted of randomly oriented crystals with a total mass of 32.3 mg for **1**, 19.4 mg for **2** and 51.0 mg for **3**. A gel cap and plastic straw were used as the sample holder during the measurements. Magnetization versus temperature measurements were run from 2 to 300 K. The sample was zero-field cooled to 2 K before a measuring field of 1000 G was applied and the data set was then taken while warming the sample from the lowest temperature. Magnetization versus field measurements were performed at 2 K from 0 to 50 kG. The background signals arising from the gel cap and straw were measured independently and subtracted from the results. The diamagnetic contribution of each sample, estimated from Pascal's constants ($\chi_D=-446\times10^{-6}$ emu mol^{-1} for **1** and **2** and $\chi_D=-516\times10^{-6}$ emu mol^{-1} for **3**), was also subtracted from the results [18,19].

ESR spectra were recorded with a Bruker (Billerica, MA) ER 200D spectrometer modified with a digital signal channel and digital field controller.

3. Results and discussion

3.1. Compound synthesis

The network coordination polymers **1**, **2** and **3** were synthesized by the direct combination of 1 equiv. of the perchlorate salt of Ni(II), Co(II) or Cu(II) with 3 equiv. of 4,4′-bipy in solution. The product contains more than 3 equiv. of 4,4′-bipy, some present as enclathrated guest molecules in addition to the coordinated ligands. It should be noted that small changes in the metal–bipy stoichiometry (for example, by using 2.5 or 3.5 equiv. of bipy instead of 3 equiv.) always produced crystalline samples of the same products.

Since the 4,4′-bipy ligand is poorly soluble in water, hydrothermal conditions are essential for the crystallization of **1** and **2** where the metal–bipy suspension is dissolved by the high temperature (150 °C) and pressure conditions within the vessel. In order to prevent the formation of unwanted side products, such as high oxidation state metal oxides, particularly with cobalt, the reaction mixture was heated for no longer than 5 days, purged with argon gas, and treated with a small amount of ethanol (acting as a mild reducing agent). The products are sensitive to loss of solvent and become opaque within a few hours upon exposure to air.

Single crystals of **3** were obtained under normal laboratory conditions by crystallization from DMSO. Attempts employing hydrothermal synthesis resulted in the formation of impure powders. Crystalline products

of **3** were obtained only after several weeks of slow evaporation of DMSO. During the first 2 to 3 weeks of crystallization, small blue blocks first appear followed by the crystallization of blue hexagonal plates of **3** after an additional month or more. The initial blue blocks were determined to be an extended three-dimensional Cu(II)-4,4′-bipyridine network of formula $[Cu_2(4,4'\text{-bipy})_5(DMSO)_3(ClO_4)][ClO_4]_3\cdot 3DMSO\cdot H_2O$ with both rectangular and hexagonal channels extending throughout the solid [20]. Reducing the Cu^{2+}:4,4′-bipy ratio in the reaction mixture favors formation of **3**, while increasing the ratio favors the crystallization of the 3D network. Unlike **1** or **2**, crystals of **3** do not appear to be sensitive to loss of solvent.

3.2. Description of the structures

Crystallographic and structural refinement data for **1**, **2** and **3** are listed in Table 1. Selected bond angles and distances for **1**, **2** and **3** are given in Tables 2–4, respectively.

3.2.1. $[Ni(4,4'\text{-bipy})_3(H_2O)_2](ClO_4)_2\cdot 1.4(4,4'\text{-bipy})\cdot 3(H_2O)$ (**1**)

The crystal structure of **1** consists of one-dimensional $[Ni(4,4'\text{-bipy})_3(H_2O)_2]^{2+}$ chains that pack to form layers in the solid state. The metal centers are six-coordinate, with the coordination sphere consisting of four pyridyl nitrogen donors from each of four 4,4′-bipy ligands and two oxygen atoms from ligated water molecules (Fig. 1). Two 4,4′-bipy ligands bridge to neighboring metal ions to form infinite *trans*-linear chains along the crystallographic *c*-axis (Fig. 2) with a Ni–Ni distance of 11.41 Å. The two Ni–N(bridging) bond distances on each metal are slightly different. Along these chains, the pyridyl rings of each bridging 4,4′-bipy ligand are not coplanar, but twisted at an angle of 29.7°. The remaining coordinated 4,4′-bipy ligands, perpendicular to the chains, are monodentate leading to metal:bipy stoichiometry within the framework of 1:3. Unlike the bridging 4,4′-bipy groups, the pyridyl rings of the terminal ligands are not twisted and these ligands π-stack with terminal bipy ligands from adjacent chains. As shown in Fig. 2(a), the chains are spaced by *b*/2 units and pack to form sheets within the crystallographic *bc*-plane. The face-to-face distance between the overlapping 4,4′-bipy groups is ~3.7 Å. Hydrogen-bonding interactions

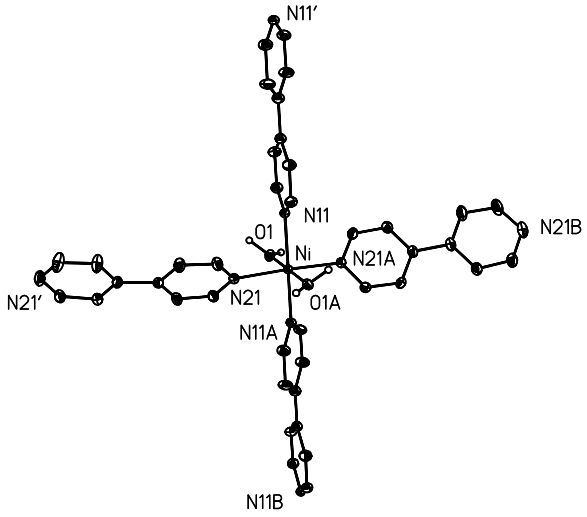

Fig. 1. The coordination environment of the metal center in **1**. Each Ni(II) ion is in a distorted octahedral environment coordinated equatorially by four 4,4′-bipyridine ligands (two bridging and two terminal) and axially by two water molecules. All hydrogen atoms have been omitted for clarity. All non-hydrogen atoms are represented by thermal ellipsoids drawn to encompass 30% of electron density.

Table 1
Summary of Crystallographic Data for **1**, **2**, and **3**

Empirical formula	$C_{44}H_{44.8}Cl_2N_{8.8}NiO_{13}$	$C_{44}H_{45.8}Cl_2N_{8.8}CoO_{13}$	$C_{54}H_{52}Cl_2N_{10}CuO_{10}S_2$
Formula weight	1022.91	1023.12	1199.62
Crystal system	monoclinic	monoclinic	monoclinic
Space group	*C*2/*c*	*C*2/*c*	*Cc*
Unit cell dimensions			
a (Å)	17.5696(8)	17.614(2)	19.0931(9)
b (Å)	11.4101(5)	11.514(1)	11.1949(5)
c (Å)	24.479(1)	24.604(2)	25.607(1)
α (°)	90	90	90
β (°)	93.065(1)	92.448(2)	94.810(1)
γ (°)	90	90	90
V (Å^3)	4900.4(4)	4985.6(9)	5454.0(4)
Z	4	4	4
T (K)	173(2)	173(2)	173(2)
λ(Mo Kα) (Å)	0.71073	0.71073	0.71073
ρ_{calc} (g cm^{-3})	1.408	1.384	1.461
μ (cm^{-1})	5.76	5.21	6.44
R [a] (R_w [b])	0.0709 (0.2069)	0.0736 (0.2173)	0.0466 (0.1179)

[a] $R = \Sigma||F_o|-|F_c||/\Sigma|F_o|$.
[b] $R_w = \Sigma[(|F_o|-|F_c|)w^{1/2}]/\Sigma[|F_o|w^{1/2}]$.

Table 2
Selected bond lengths (Å) and bond angles (°) for **1**

Bond lengths			
Ni–O1	2.060(3)	Ni–N21	2.115(3)
Ni–N11	2.127(4)		
Bond angles			
O1–Ni–O1A	179.82(15)	N11–Ni–O1	89.91(7)
N11–Ni–N11A	180.000	N11A–Ni–N21	91.40(7)
N21–Ni–N21A	177.20(15)	N11A–Ni–O1	90.09(7)
N11–Ni–N21	88.60(7)	N21–Ni–O1	92.44(11)

Symmetry transformation used to generate equivalent atoms: A: $-x, y, -z+3/2$.

Table 3
Selected bond lengths (Å) and bond angles (°) for **2**

Bond lengths			
Co–O1	2.061(3)	Co–N11A	2.232(4)
Co–O1A	2.061(3)	Co–N21	2.168(3)
Co–N11	2.180(4)	Co–N21A	2.168(3)
Bond angles			
O1–Co–O1A	178.68(14)	N11–Co–O1	90.66(7)
N11–Co–N11A	180.000	N11A–Co–N21	91.81(7)
N21–Co–N21A	176.37(14)	N11A–Co–O1	89.34(7)
N11–Co–N21	88.19(7)	N21–Co–O1	92.17(11)

Symmetry transformation used to generate equivalent atoms: A: $-x, y, -z+3/2$.

between the uncoordinated nitrogen atoms of the terminal bipy ligands with water molecules on adjacent chains, combined with the π-stacking, act to hold the chains together within the sheets.

Adjacent chains define hydrophobic, rectangular cavities enclosed by four nickel ions at the corners and six bipy ligands, one bridging bipy on edges along the chain and two each on edges between the chains. The dimensions of the rectangles are $b/2 \times c$ and, if the van der Waals radii of the ligated bipy carbon atoms are

Table 4
Selected bond lengths (Å) and bond angles (°) for **3**

Bond lengths			
Cu–O1	2.396(3)	Cu–N1′	2.060(2)
Cu–O2	2.376(3)	S1–O1	1.507(3)
Cu–N1	2.049(2)	S2–O2	1.488(3)
Cu–N2	2.025(4)	S2′–O2	1.347(11)
Cu–N3	2.033(3)		
Bond angles			
N1–Cu–N1′	178.39(18)	N3–Cu–O1	87.78(14)
N2–Cu–N3	179.25(19)	N1′–Cu–O1	89.13(15)
O1–Cu–O2	178.17(15)	N1–Cu–O2	90.01(14)
N1–Cu–N2	91.09(14)	N2–Cu–O2	86.81(14)
N1–Cu–N3	89.03(14)	N3–Cu–O2	93.93(14)
N1′–Cu–N2	90.51(15)	N1′–Cu–O2	90.21(16)
N1′–Cu–N3	89.36(15)	S1–O1–Cu	141.6(2)
N1–Cu–O1	90.69(14)	S2–O2–Cu	145.9(2)
N2–Cu–O1	91.49(14)	S2′–O2–Cu	154.1(2)

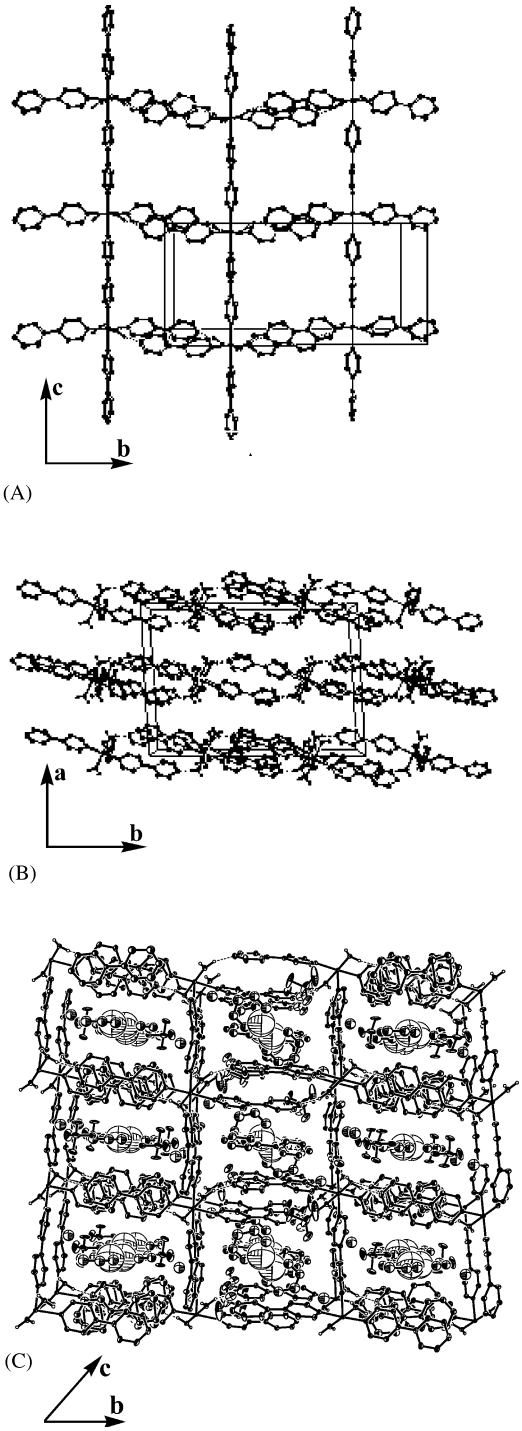

Fig. 2. (A) A portion of a two-dimensional sheet of **1** formed within the crystallographic *bc*-plane by interaction of the terminal 4,4′-bipyridine ligands perpendicular to the chains. (B) The structure of **1** within the crystallographic *ab*-plane depicting the relative positions of the sheets. All guest molecules and hydrogen atoms (except from coordinated water molecules) have been omitted for clarity. (C) The hydrophobic channels containing enclathrated guest molecules and counterions that extend throughout the solid parallel to the crystallographic *b*-axis in **1**. All hydrogen atoms (except from coordinated water molecules) have been omitted for clarity.

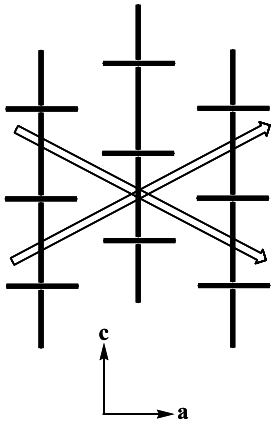

Fig. 3. Schematic depicting the solid-state structure of **1**, **2** or **3** within the crystallographic *ac*-plane. Adjacent sheets within the *bc* plane pack in registry along the *b*-axis with, but are offset by $\frac{1}{2}$ step along the *c*-axis, resulting in a series of oblique channels extending throughout the solid perpendicular to the *b*-axis, as indicated by the arrows.

approximated as 1.7 Å, the effective size of the cavities is approximately 9.7 Å × 10.7 Å. The space surrounding the cavities and between the sheets is occupied by enclathrated guest molecules and counterions, acting to prevent the interpenetration of adjacent sheets. The sheets pack along the crystallographic *a*-axis with a spacing of *a*/2 to complete the structure in the third dimension (Fig. 2(b)). Although the sheets align in registry along the *b*-axis, they are offset by *c*/2, resulting in alignment of the hydrophobic cavities (Fig. 2(c)) to form oblique channels within the *ac* plane, as illustrated in Fig. 3.

The channels within the framework host are not empty, but occupied by enclathrated guest molecules and counterions. These lattice guests are extensively disordered throughout the solid, thus leading to the rather high final refinement value in the structural solution. Approximately 1.5 crystallographically inequivalent, uncoordinated bipy molecules, each disorderd about centers of inversion, are present per asymmetric structural unit. The specific quantity 1.4 in the formula provides the best structural solution and reflects a positional disorder between the perchlorate counterions and the pyridyl group of an enclathrated bipy between the sheets. Bipy molecules present between the sheets stack approximately parallel to the terminal bipy ligands coordinating the chains, while the hydrophobic cavities also contain highly disordered bipy molecules. The perchlorate counterions, also disordered within the lattice, are positioned between the sheets in close proximity to the bipy guests. Extensive hydrogen bonding interactions between the lattice waters and the coordinated waters, perchlorate ions, and bipy guests are present throughout the channels.

The Ni–bipy bonds along the chain axis are axially elongated, despite the presence of the weaker-field water ligands. This feature may result from a combination of steric interactions with the terminal bipy ligands and strengthening of the water ligand field by hydrogen bonds to non-coordinating nitrogen atoms from bipy ligands on adjacent chains.

The structure of **1** bears close resemblance to a compound reported by Yaghi and coworkers, $[Ni(4,4'\text{-bipy})_{2.5}(H_2O)_2](ClO_4)_2\cdot 1.5(4,4'\text{-bipy})\cdot 2(H_2O)$ [9], that has been described as a molecular railroad where similar one-dimensional chains are dimerized with crosslinking bipy ligands. Both structures incorporate bridging and terminal 4,4′-bipy ligands as well as 4,4′-bipy enclathrated in channels. In the railroad structure, 4,4′-bipy ligands bridge Ni^{2+} ions to form the legs and rungs of a ladder with each metal ion also coordinated by a terminal bipy. In **1**, each metal ion is coordinated by two terminal bipy ligands and is only bridged along the chain axis.

3.2.2. $[Co(4,4'\text{-bipy})_3(H_2O)_2](ClO_4)_2\cdot 1.4(4,4'\text{-bipy})\cdot 3(H_2O)$ (**2**)

Other than substituting the metal center Co^{2+} for Ni^{2+} and small differences in characteristic bond angles and distances, the structure of **2** is virtually identical to **1** and thus no pictures or description is given. The structure of **2** resembles the *trans*-1D chain compounds reported by Jacobson and coworkers, $[Co(4,4'\text{-bipy})(SO_4)(H_2O)_2]\cdot 2(H_2O)$ and $[Co(4,4'\text{-bipy})(Cl)_2(DMSO)_2]$ [10] where the solvent molecules and counterions, not terminal bipy ligands, occupy the non-bridging coordination sites on the metal centers.

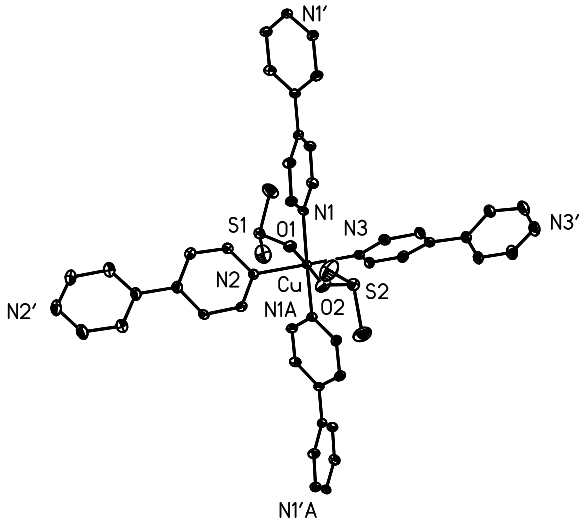

Fig. 4. The coordination of the metal center in **3**. Each Cu(II) ion is in a distorted octahedral environment coordinated equatorially by four 4,4′-bipyridine ligands (two bridging and two terminal) and axially by two dimethyl sulfoxide molecules. All hydrogen atoms as well as the disorder present within one of the DMSO ligands have been omitted for clarity. All non-hydrogen atoms are represented by thermal ellipsoids drawn to encompass 30% of electron density.

3.2.3. $[Cu(4,4'\text{-bipy})_3(DMSO)_2](ClO_4)_2 \cdot 2(4,4'\text{-bipy})$ (3)

Although **3** is structurally related to **1** and **2**, some important differences are present. Each copper ion is six-coordinate, with four pyridyl nitrogen donors from each of four 4,4′-bipyridine ligands and two oxygen atoms from ligated DMSO molecules (Fig. 4). One DMSO ligand per metal site is disordered in the sulfur atom. Two bipy ligands bridge the metal ions to form infinite *trans*-linear chains along the crystallographic *c*-axis with a Cu–Cu distance of 11.20 Å. Along these chains, the pyridyl rings from each bridging bipy ligand are twisted at an angle of 61.4° with respect to one another, considerably larger than in **1** or **2**. The remaining coordinated bipy ligands, perpendicular to the chains, are monodentate as in **1** and **2**. The pyridyl rings on each of these terminal bipy ligands are slightly twisted 11.9° with respect to each other. The Cu–N bond distances from the bridging bipy ligands are slightly longer than those of the terminal bipy groups. The chains are spaced by $b/2$ and pack to form layered sheets within the crystallographic *bc*-plane via offset π overlap interactions between the terminal bipy ligands from adjacent chains. The face-to-face distance between these overlapping bipy groups is ~ 3.8 Å. However, unlike in **1** and **2**, no significant hydrogen-bonding interactions between the chains are present. Also unlike **1** or **2**, the Cu–O bonds are longer that the Cu–N bonds in **3**. The DMSO molecules are weaker field ligands compared to the bipy ligands and, in combination with the Jahn–Teller effect, the solvent molecules are located on the axially distorted coordination sites.

As in **1** and **2**, hydrophobic rectangular cavities are present within the framework of dimensions $b/2 \times c$ with effective size of 9.5 Å × 11.27 Å, when accounting for the van der Waals surface, slightly larger than the cavities present in **1** and **2**. As shown in Fig. 5, the sheets pack along the crystallographic *a*-axis with a spacing of $a/2$ to complete the structure in the third dimension, but the spacing between the sheets in **3** is larger than in **1** or **2**. The methyl groups from the coordinated DMSO molecules interact with those on adjacent sheets, whereas, the water molecules between the sheets in **1** and **2** are too small and far apart from each other to interact.

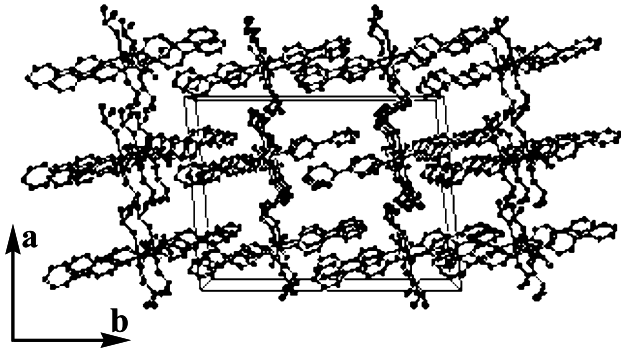

Fig. 5. The structure of **3** within the crystallographic *ab*-plane depicting the relative positions of each sheet. All guest molecules and hydrogen atoms have been omitted for clarity.

The lattice guests are less disordered in **3** relative to **1** and **2**, resulting in a better structural refinement. Two crystallographically inequivalent, uncoordinated 4,4′-bipy molecules are present per asymmetric structural unit, with one disordered about a center of inversion. Both lattice bipy's are present between the sheets. The perchlorate anions, also disordered within the lattice, are found between the sheets in close proximity to the terminal bipy ligands perpendicular to the framework chains. No non-coordinated lattice DMSO molecules are present, and unlike in **1** and **2**, there is no significant hydrogen bonding between guest molecules, counter-ions, and coordinated solvent molecules.

3.3. Thermal properties

Compounds **1** and **2** are unstable in air due to loss of enclathrated guest molecules. The compounds can be kept in humid environment or under solvent, but both compounds discolor and change texture if left in laboratory atmosphere. Thermogravimetric analysis and thermal desorption mass spectrometry show the gradual loss of water followed by uncoordinated bipyridine [20]. Initial mass loss (5%) between room temperature and 56 °C corresponds to three equivalents of water, presumably corresponding to guest water molecules in the chemical formula. Water continues to come off up to near 150 °C. Above 85 °C, bipyridine is lost continuously up to approximately 250 °C. The cobalt analogue, **2**, undergoes similar guest molecule loss.

In contrast to **1** and **2**, the copper compound **3** is stable in air at room temperature. Without solvent molecule guests, it does not experience the same decomposition process. The first mass decrease observed by TGA occurs above 100 °C and corresponds to loss of guest bipyridine molecules.

3.4. Magnetic properties

The magnetic properties of **1** and **2** are similar in the sense that weak exchange interactions are present between the metal centers. The Ni^{2+} ions of **1** form chains of Heisenberg $S = 1$ spins that experience single-ion, D, and in-plane, E, anisotropies, and this analysis is presented later in this section. On the other hand, the Co^{2+} ions of **2** form chains of Ising spins that assume an effective $S = 1/2$ spin state at temperatures below approximately 30 K as a result of zero field splitting. Due to the significant anisotropy associated with these Ising spins, a complete analysis of their magnetic behavior requires data from single crystals in different

orientations with respect to the measuring magnetic field [18,19,21]. Although experiments were performed with powder specimens, qualitatively the Co^{2+} spins exhibit behavior consistent with weak magnetic exchange, and no long-range ordering is observed down to 2 K. A full discussion of the magnetic properties of **2** is given elsewhere [20].

For the case of the Cu^{2+} ions of **3**, the room temperature susceptibility, $1.69\mu_B$, correlates well with the value expected for uncoupled, $S = 1/2$ metal centers. The temperature dependence of the magnetic susceptibility at 1 kG is fit well by the Curie law using a g-value of 2.06, as determined from a room temperature EPR measurement. The field dependence of the magnetization at 2 K and up to 50 kG is also fit well by the $S = 1/2$ Brillouin function, which describes non-interacting magnetic spins [18,19]. Consequently, the Cu(II) centers in **3** behave as a chain of non-interacting, $S = 1/2$ metal centers that are uncoupled even at 2 K. The large dihedral angle between the pyridyl rings on the bridging bipy ligands may disrupt the superexchange pathway and likely accounts for the lack of any observed exchange interaction. A detailed presentation of the magnetic data is given elsewhere [20].

The magnetic susceptibility for **1**, as well as its inverse susceptibility, at 1 kG and over the temperature range of 2–300 K are plotted in Fig. 6, while the magnetization, M, at 2 K and up to 50 kG is presented in Fig. 7. The room temperature susceptibility, 3.09 μ_B, correlates well with the value expected for uncoupled, $S = 1$ metal centers. The temperature dependence of the inverse susceptibility between 5 and 50 K can be fit by a simple Curie–Weiss Law, $\chi^{-1}(T) = (T+\theta)/C$, where the Curie constant $C = N(g\mu_B)^2 S(S+1)/(3k_B)$. The results of the fit yield a Weiss temperature $\theta = -2$ K, consistent with

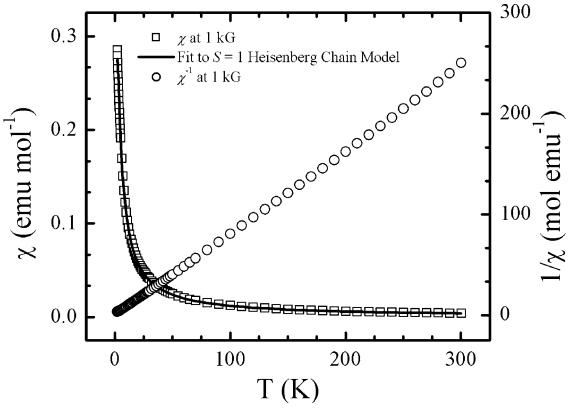

Fig. 6. Molar magnetic susceptibility (χ) and inverse molar magnetic susceptibility ($1/\chi$) measured in 1 kG from 2 to 300 K for **1**. The data have been corrected for background signals arising from the sample container as well as diamagnetic contributions. The fit to the data is shown by the solid line.

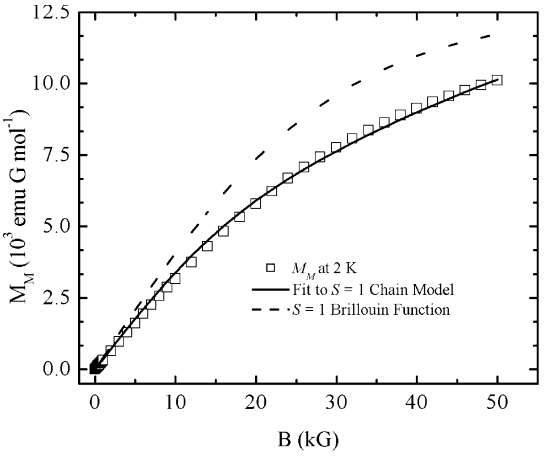

Fig. 7. Molar magnetization (M) at 2 K from 0 to 50 kG for **1**. The data have been corrected for background signals arising from the sample container. The results of fitting to Eq. (1), using values of the parameters included in the text, are shown as the solid line. For comparison, the $S = 1$ Brillouin function (appropriate for non-interacting spins) is given by the dashed line.

weak antiferromagnetic interactions along the chains, and the value for the Curie constant provides $g = 2.20$.

Since the structure of **1** consists of chains of Ni(II) ions covalently bridged by 4,4′-bipy ligands, a $S = 1$ linear chain model incorporating both zero field splitting and exchange parameters is appropriate to fit the magnetic data, and an analysis beyond the Curie–Weiss fit was attempted. Only exchange interactions along the chains were considered and coupling between the chains was ignored since interchain interactions are noncovalent. The Heisenberg model is an appropriate starting point since octahedral Ni(II) complexes have nearly isotropic g-factors and the Hamiltonian may be written as

$$\mathrm{H} = -J\sum_i S_i S_{i+1} + D\sum_i (S_i^z)^2 + E\sum_i [(S_i^x)^2 - (S_i^y)^2] + g\mu_B B\sum_i S_i \quad (1)$$

where J is the exchange interaction constant, D is the single-ion anisotropy, E is the in-plane anisotropy, and B is the applied magnetic field.

The temperature dependence of the low field susceptibility may be fit using the expressions derived by Papanicolaou and Spathis [22], and the results of this analysis, when using $g = 2.20$ [18,23], are given by the solid line in Fig. 6, where $J/k_B = -0.9$ K, $D/k_B = 4.7$ K, and $E = 0$. The small, negative coupling constant is consistent with weak antiferromagnetic exchange along the chains. Since these measurements were performed on randomly oriented samples, the sign of D cannot be unambiguously determined [19]. The $D/|J|$ ratio of about 5 indicates that **1** is an example of a large $|D|/J$

system with strong planar anisotropy [22,24–26]. An analysis of the magnetization of **1** as a function of applied field at 2 K is also consistent with this conclusion [20].

The delocalized π orbital system of 4,4′-bipyridine should allow the ligand to effectively mediate superexchange interactions when covalently bridging paramagnetic centers. Furthermore, the coupling is expected to be antiferromagnetic as explained by a spin-polarization mechanism for the propagation of exchange interactions [16]. The magnitude of the coupling constant in **1** is, however, small ($J/k_B = -0.9$ K), but consistent with the coupling constants measured for other similar bipy bridged complexes [Ni(Et-XA)$_2$(4,4′-bipy-)]·0.5(EtOH)·($CHCl_3$) (Et-XA = ethylcarbonadithiolate) [11], [Mn(hfac)$_2$(4,4′-bipy)] (hfac = hexafluoroacetylacetonato) [13], [Cu_2(tren)$_2$(4,4′bipy)](BPH_4)$_4$ [27], [Cu_2(dien)$_2$(4,4′-bipy)(ClO_4)$_2$](ClO_4)$_2$ [28], and [Mn-μ-(4,4′-bipy)(4,4′-bipy)(NCS)$_2$(H_2O)$_2$]$_n$ [29]. The small exchange is partially a result of twisting about the central C–C bond of the bridging bipy ligand and is consistent with the coupling constants measured.

4. Conclusions

Three new hybrid organic–inorganic coordination polymers have been isolated and characterized. These materials consist of chains of transition metal ions (Ni(II), Co(II), and Cu(II)) bridged by 4,4′-bipyridine spacer ligands. The chains pack to form two-dimensional, non-interpenetrated sheets with hydrophobic, rectangular cavities present within the framework. The sheets, in turn, pack to form a three-dimensional structure with oblique channels containing enclathrated guest molecules and counterions extending throughout the solid. These enclathrated guests are easily lost suggesting that the samples are thermally unstable. Magnetic measurements show effectively no exchange interactions between the paramagnetic metal centers.

Coordination polymers with hydrophobic cavities and channels extending throughout the solid-state structure have received much attention due to their ability to act as molecular sieves with size and shape specificity and catalytic substrates [1,30,31]. Compounds **1**, **2** and **3** are clearly examples of network solids with cavities and channels that prefer to enclathrate hydrophobic guests (uncoordinated bipy molecules). The ability of these coordination polymer hosts to exchange guests is currently under study.

5. Supplementary material

Crystallographic data for the structural analysis have been deposited with the Cambridge Crystallographic Data Centre, CCDC Nos. 204397–204399 for compounds **1**–**3**, respectively. Copies of this information may be obtained free of charge from The Director, CCDC, 12 Union Road, Cambridge, CB2 1EZ, UK (fax: +44-1223-336033; e-mail: deposit@ccdc.cam.ac.uk or www: http://www.ccdc.cam.ac.uk).

Acknowledgements

This work was partially supported by the National Science Foundation through grant DMR 9900855 (DRT). Partial support from the Petroleum Research Fund, administered by the ACS, is gratefully acknowledged (M.W.M. and D.R.T.). K.A.A. wishes to acknowledge the National Science Foundation and the University of Florida for funding of the purchase of the X-ray equipment. We also thank Dr. Kathryn R. Williams for assistance in the TGA measurements and Dr. Martin Orendac for independent verification of some of the fitting results.

References

[1] M. Fujita, Y.J. Kwon, S. Washizu, K. Ogura, Inorg. Chem. 116 (1994) 1151.
[2] J.Y. Lu, M.A. Lawandy, J. Li, T. Yuen, C.L. Lin, Inorg. Chem. 38 (1999) 2695.
[3] D. Hagrman, R.P. Hammond, R. Haushalter, J. Zubieta, Chem. Mater. 10 (1998) 2091.
[4] D. Hagrman, C. Zubieta, D.J. Rose, J. Zubieta, R.C. Haushalter, Angew. Chem. Int. Ed. Engl. 36 (1997) 8.
[5] P. Losier, M.J. Zaworotko, Angew. Chem. Int. Ed. Engl. 35 (1996) 2779.
[6] K.N. Power, T.L. Hennigar, M.J. Zaworotko, New. J. Chem. (1998) 177.
[7] K. Biradha, K.V. Domasevitch, B. Moulton, C. Seward, M.J. Zaworotko, Chem. Commun. (1999) 1327.
[8] L.R. MacGillivray, R.H. Groeneman, J.L. Atwood, J. Am. Chem. Soc. 120 (1998) 2676.
[9] O.M. Yahgi, H. Li, T.L. Groy, Inorg. Chem. 36 (1997) 4292.
[10] J. Lu, C. Yu, T. Niu, T. Paliwala, G. Crisci, F. Somosa, A.J. Jacobson, Inorg. Chem. 37 (1998) 4637.
[11] R.G. Xiong, C.M. Liu, X.Z. You, Polyhedron 16 (1997) 2667.
[12] J. Lu, T. Paliwala, S.C. Lim, C. Yu, T. Niu, A.J. Jacobson, Inorg. Chem. 36 (1997) 923.
[13] H. Shen, D. Liao, Z. Jiang, S. Yan, B. Sun, G. Wang, X. Yao, H. Wang, Polyhedron 17 (1998) 1953.
[14] A.J. Blake, S.J. Hill, P. Hubberstey, W.S. Li, J. Chem. Soc., Dalton Trans. (1997) 913.
[15] M.L. Tong, B.H. Ye, J.W. Cai, X.M. Chen, S.W. Ng, Inorg. Chem. 37 (1998) 2645.
[16] J.A. McCleverty, M.D. Ward, Acc. Chem. Res. 31 (1998) 842.
[17] G.M. Sheldrick, SHELXTL6, 6 ed., Bruker-AXS, Madison, WI, 2000.
[18] R.L. Carlin, Magnetochemistry, 1st ed., Springer-Verlag, Berlin, 1986.
[19] O. Kahn, Molecular Magnetism, VCH Publishers, New York, 1993.

[20] J.D. Woodward, Chemical and physical characterization of hybrid organic–inorganic low-dimensional coordination polymers, PhD thesis, University of Florida, Gainesville, 2002.
[21] W.M. Hatfield, W.E. Estes, W.E. Marsh, M.W. Pickens, L.W. Harr, R.R. Weller, in: J.S. Miller (Ed.), The Synthesis and Static Magnetic Properties of First-Row Transition Metal Compounds with Chain Structures, Plenum Press, New York, 1983.
[22] N. Papanicolaou, P.N. Spathis, Phys. Rev. B 52 (1995) 16001.
[23] A. Abragam, B. Bleaney, Electron Paramagnetic Resonance of Transition Ions, Oxford University Press, London, 1970.
[24] M. Orendac, A. Orendacova, J. Cernak, A. Feher, P.J.C. Signore, M.W. Meisel, S. Merah, M. Verdaguer, Phys. Rev. B 52 (1995) 3435.
[25] M. Orendac, S. Zvyagin, A. Orendacova, M. Sieling, B. Luthi, A. Feher, M.W. Meisel, Phys. Rev. B 60 (1999) 4170.
[26] M. Orendac, E. Cizmar, J. Cernak, A. Feher, M.W. Meisel, K.A. Abboud, S. Zvyagin, M. Sieling, T. Rieth, B. Luthi, Phys. Rev. B 61 (2000) 3323.
[27] M.S. Haddad, D.N. Hendrickson, J.P. Cannady, R.S. Drago, D.S. Bieksza, J. Am. Chem. Soc. 101 (1979) 898.
[28] M. Julve, M. Verdauger, J. Faus, F. Tinti, J. Moratal, A. Monge, E. Guiterrez-Puebla, Inorg. Chem. 26 (1987) 3520.
[29] M.X. Li, G.Y. Xie, Y.D. Gu, Polyhedron 14 (1995) 1235.
[30] O.M. Yaghi, H. Li, C. Davis, D. Richardson, T.L. Groy, Acc. Chem. Res. 32 (1998) 474.
[31] O.M. Yaghi, G. Li, H. Li, Nature 378 (1995) 703.